Title
Formation of fulvene in the reaction of C2H with 1,3-butadiene

Authors
Lockyear, Jessica F
Fournier, Martin
Sims, Ian R
et al.

Publication Date
2015-02-01

DOI
10.1016/j.ijms.2014.08.025

Peer reviewed

International Journal of Mass Spectrometry 378 (2015) 232–245

Contents lists available at ScienceDirect

International Journal of Mass Spectrometry

journal homepage: www.elsevier.com/locate/ijms

Formation of fulvene in the reaction of C_2H with 1,3-butadiene

Jessica F. Lockyear [a,1], Martin Fournier [b,c], Ian R. Sims [b], Jean-Claude Guillemin [c], Craig A. Taatjes [d], David L. Osborn [d], Stephen R. Leone [a,*]

[a] Departments of Chemistry and Physics, University of California at Berkeley, and Lawrence Berkeley National Laboratory, Berkeley, CA 94720, USA
[b] Institut de Physique de Rennes, UMR CNRS-UR1 6251, Université de Rennes 1, 263 Avenue du Général Leclerc, 35042 Rennes CEDEX,France
[c] Ecole Nationale Supérieure de Chimie de Rennes, CNRS UMR 6226, 11 Allée de Beaulieu, CS 50837, 35708 Rennes CEDEX 7, France
[d] Combustion Research Facility, Mailstop 9055, Sandia National Laboratories, Livermore, CA 94551-0969, USA

ARTICLE INFO

Article history:
Received 30 May 2014
Received in revised form 21 July 2014
Accepted 11 August 2014
Available online 20 August 2014

Keywords:
Combustion chemistry
Astrochemistry
Fulvene
Benzene
Polycyclic aromatic Hydrocarbons
Photoionization

ABSTRACT

Products formed in the reaction of C_2H radicals with 1,3-butadiene at 4 Torr and 298 K are probed using photoionization time-of-flight mass spectrometry. The reaction takes place in a slow-flow reactor, and products are ionized by tunable vacuum-ultraviolet light from the Advanced Light Source. The principal reaction channel involves addition of the radical to one of the unsaturated sites of 1,3-butadiene, followed by H-loss to give isomers of C_6H_6. The photoionization spectrum of the C_6H_6 product indicates that fulvene is formed with a branching fraction of (57 ± 30)%. At least one more isomer is formed, which is likely to be one or more of 3,4-dimethylenecyclobut-1-ene, 3-methylene-1-penten-4-yne or 3-methyl-1,2-pentadien-4-yne. An experimental photoionization spectrum of 3,4-dimethylenecyclobut-1-ene and simulated photoionization spectra of 3-methylene-1-penten-4-yne and 3-methyl-1,2-pentadien-4-yne are used to fit the measured data and obtain maximum branching fractions of 74%, 24% and 31%, respectively, for these isomers. An upper limit of 45% is placed on the branching fraction for the sum of benzene and 1,3-hexadien-5-yne. The reactive potential energy surface is also investigated computationally. Minima and first-order saddle-points on several possible reaction pathways to fulvene + H and 3,4-dimethylenecyclobut-1-ene + H products are calculated.

Published by Elsevier B.V.

1. Introduction

There are many parallels between combustion chemistry and the chemistry of planetary atmospheres and interstellar space. In these environments, reactions of radicals with hydrocarbons lead to molecular-weight growth and formation of polycyclic aromatic hydrocarbons (PAHs). Further, it is often the same radicals that are thought to be responsible for these important processes in such varied environments. PAHs are significant in astrochemistry because they are complex molecules whose formation may give us clues to the chemistry of a prebiotic earth [1,2]. In combustion, the mechanism of PAH formation is investigated in order to curtail it, because PAHs and soot emitted from combustion engines [3–5] are significant pollutants.

Benzene (C_6H_6), the simplest closed-shell aromatic ring, is likely to be a key primary reactant in PAH chemistry and it has been detected in the circumstellar envelopes [6,7], the atmosphere of Titan [2,8] and in numerous combustion and flame studies [9,10]; thus, many reactions have been postulated to explain its formation. In addition, it is vital to know the pre-cyclization chemistry as well as the critical ring-forming reactions to understand the generation of PAHs [4]. In combustion environments, propargyl (C_3H_3) recombination is generally thought to be one of the main benzene formation pathways [4,11–13]. However, several studies have shown that benzene is a minor, or non-existent, product of propargyl recombination at low temperatures and pressures [12,14]. The $C_3H_3 + C_3H_3$ route to C_6H_6 can only proceed by relatively inefficient radiative association in the very low pressures of astrochemical environments and so alternative mechanisms must be invoked. Another popular candidate for benzene formation is the reaction between the 1,3-butadien-1-yl radical (n-C_4H_5) and acetylene (C_2H_2), which undergoes an addition–elimination reaction to yield $C_6H_6 + H$ [3,4,15]. However, there are conflicting accounts of the importance of C_4H_5 in benzene formation, not the least of which is that 1,3-butadien-2-yl (i-C_4H_5) is more stable than n-C_4H_5, but it is preferable to have the latter for facile benzene formation [4]. In 1989 Westmoreland et al. outlined 18 suggested pathways to benzene formation in combustion [9]. Despite all current and past efforts, even the most rigorous combustion

* Corresponding author. Tel.: +1 510 643 5467.
E-mail addresses: jess.lockyear@gmail.com (J.F. Lockyear), srl@berkeley.edu (S.R. Leone).
[1] Tel.: +1 5103295313.

http://dx.doi.org/10.1016/j.ijms.2014.08.025
1387-3806/Published by Elsevier B.V.

models available are unable to accurately predict concentrations of species such as C_6H_6, C_5H_6, and C_8H_6[16]. For example, the concentrations of 1-butyne (CH_3CH_2CCH), 2-butyne (CH_3CCCH_3), 1,3-butadiene ($CH_2CHCHCH_2$), C_4H_5, C_4H_4, C_4H_3 and 1,3-butadiyne (C_4H_2) from a butanol flame experiment are not well replicated by the associated model and the authors of this study state that this discrepancy arises because the base C_4 chemistry has not been thoroughly validated for recombination reactions that lead to highly unsaturated C_4 and larger hydrocarbons [16].

A promising species in the search for cyclization reactions is the ethynyl radical (C_2H), which is abundant in many astronomical environments [17–19]. The C_2H radical readily undergoes barrierless addition–elimination reactions with unsaturated hydrocarbons [20]. The fact that these reactions are barrierless is important in low temperature astrochemical environments, where entrance barriers are difficult or impossible to overcome. Reactions of C_2H have been implicated in the generation of long chain polyynes that have been detected in the interstellar medium (ISM) [6,21,22]. Moreover, the eliminated moiety in the addition–elimination reactions of this radical is often a hydrogen atom, meaning that C_2H reacting with C_4H_6 yields isomers of C_6H_6 + H. Thus, C_2H has been suggested by Kaiser and co-workers to be a critical species in benzene formation in the ISM [23]. Although in combustion environments C_2H is present at concentrations that are too small to make a substantial contribution to soot formation, C_2H is formed *via* several reactions: between the hydroxyl radical (OH) and C_2H_2 to form water (H_2O) and C_2H [4], between C_3H_3 and oxygen atoms (O) to form formaldehyde (CH_2O) + C_2H, between C_3H_3 and methyl radicals (CH_3) to form ethyl radicals (C_2H_5) + C_2H [24], or between C_3H_3 and methylene radicals (CH_2) to form ethene (C_2H_4) + C_2H [11]. In addition, C_2H can be formed by the reaction of hydrogen atoms (H) with C_2H_2 at higher temperatures [5,25].

Recently, Mebel and co-workers have carried out an extensive *ab initio* investigation into the reactions of C_2H with unsaturated hydrocarbons, including all isomers of C_4H_6 (1,3-butadiene [23], 1,2-butadiene [20], 1-butyne and 2-butyne [26]). In a combined crossed-molecular beams and computational study, Jones et al. suggested that benzene is formed in the reaction between C_2H and 1,3-butadiene [23], at kinetic energies higher than thermal. In the crossed-molecular beams experiment products were ionized by electron impact at 80 eV, and isomer identification was achieved by examination of product translational energy distributions. The experimental part of the study indicated a branching fraction for benzene of 30%, with the other 70% of products being 1,3-hexadien-5-yne. The theoretical study found a benzene branching fraction between 40% and 20% at collision energies between 0 kJ mol^{-1} and 45 kJ mol^{-1}. To our knowledge, this is the only experimental report of the products of the C_2H + 1,3-butadiene reaction, and therefore it is valuable to investigate this reaction *via* additional methods.

The reaction of the cyano radical (CN), which is isoelectronic with C_2H, with 1,3-butadiene has also been studied [27]. Previous studies of the reactions of the isoelectronic C_2H and CN radicals with unsaturated hydrocarbons have shown that they react similarly, both in terms of reaction rate and major products [28–31]. Thus, one might expect the outcome of the CN + 1,3-butadiene reaction to provide clues to the C_2H + 1,3-butadiene reaction mechanism. CN + 1,3-butadiene proceeds *via* addition and H-elimination to yield isomers of C_5H_5N. Crossed-molecular beams experiments suggest a maximum of 3–6% pyridine and 94–97% 1-cyano-1,3-butadiene is formed under single collision conditions. Rice–Ramsperger–Kassel–Marcus (RRKM) calculations predict only 0.02% pyridine formation at 0 eV collision energy, with a maximum of 6% at the limits of the errors of the calculations [27]. If C_2H + 1,3-butadiene were analogous to CN + 1,3-butadiene, one might expect a small branching fraction for benzene, with the remainder of the products being 1,3-hexadien-5-yne.

Despite the likely importance of C_2H reactions with C_4H_6 isomers, very few other studies examining them have been published. The reasons for this are manifold, including the technique chosen to produce the C_2H radical. Generally, in flow tube experiments, C_2H is formed *via* 193 nm photolysis of C_2H_2, or occasionally 193 nm photolysis of trifluoromethylacetylene (CF_3CCH). Recent work in our group has employed 193 nm photolysis of C_2H_2 and CF_3CCH to determine the products and rates of reactions of C_2H with acetylene [32], ethene [33], propene [33], butenes [34], allene [35] and propyne [35], among others. However, polyunsaturated and acetylenic C_4 (and higher) hydrocarbons tend to absorb strongly at 193 nm, so there are concurrent photodissociation yields of radicals that can interfere with the reaction of interest or give rise to secondary reactions that complicate the analysis. Our group has reported one experimental study of C_2H with an isomer of C_4H_6, specifically 1-butyne [36], which employed 193 nm photolysis of C_2H_2 to generate the radicals and in which the contribution of products due to 1-butyne photolysis was carefully examined and accounted for. Clearly a method that avoids photodissociation of the molecular co-reactant is preferable. At 300 K, 1,3-butadiene absorbs strongly at 193 nm, but only weakly at 248 nm. Consequently, for the experimental work here, a different C_2H precursor was synthesized, bromoacetylene (BrC_2H), which photolyses efficiently at 248 nm to give Br + C_2H [37]. Details of the synthetic method are given in Section 2.

Determining the ratio between straight chain and cyclic isomer products of the title reaction is valuable for understanding astrochemical and combustion chemistry. By synthesizing bromoacetylene, an excellent C_2H precursor when photolysed at 248 nm, problems with interfering dissociative products of the 1,3-butadiene are minimized. Obtaining product masses is achieved by tunable synchrotron ionization, time-of-flight mass spectrometry. This method is a powerful multiplexed technique that allows the identification of the product isomers formed. In the following sections, the experimental techniques are described and the recorded reaction spectra are presented. These results are followed by a discussion of the extracted branching fractions and possible reaction pathways, calculated at the CBS-QB3 level. Finally, the implications of current results for our understanding of astrochemical and combustion environments are discussed.

2. Experimental details

The experimental technique comprises several components. Synthesized BrC_2H gas is mixed with 1,3-butadiene and flowed through a quartz tube housed in a vacuum chamber. Photodissociation of BrC_2H forms Br + C_2H, which react with the closed-shell 1,3-butadiene. Gases exit the reactor through a pinhole and are ionized with tunable vacuum ultra-violet light in a differentially pumped chamber. The mass-analysis of the products is carried out using a time-of-flight mass-spectrometer. Details of the spectrometer and the synthesis procedure will be given in the following sections. In addition, the computational methodologies employed for supporting interpretation of the data are also described.

2.1. Multiplexed photoionization mass spectrometer

The C_2H + 1,3-butadiene reaction takes place in a laser photolysis, slow flow reactor coupled to a multiplexed photoionization mass spectrometer at the Advanced Light Source of Lawrence Berkeley National Laboratory. Comprehensive details of the experimental apparatus are given elsewhere [38–40] and only an overview is presented here. The reactions occur inside a

quartz tube with 1.05 cm inner diameter at 4 Torr (533 Pa) and 298 K. The gas flow consists of small amounts of the C_2H radical precursor, BrC_2H, and 1,3-butadiene in a large excess of helium buffer gas. Dilutions of BrC_2H and 1,3-butadiene in helium are prepared in stainless steel cylinders with a total pressure of 2000 Torr. The gases are mixed *in situ* at the entrance of the reactor using calibrated mass flow controllers. The total flow is 100 sccm (standard cubic centimeters per minute), sufficient to completely replenish the gas in the reactor tube between consecutive laser pulses (4 Hz repetition rate). Reactor pressure is maintained with a butterfly valve after the reactor under active feedback control.

A uniform initial concentration of C_2H radicals is produced in the axial and radial directions of the reactor tube by 248 nm photolysis of BrC_2H using the unfocused beam of an excimer laser. The typical photolysis fluence inside the reaction flow tube is $\sim$70 mJ cm^{-2} in a 20 ns pulse. There is effectively no attenuation of the photon flux along the length of the flow tube due to absorption, as verified by the stable concentrations of products of photolytically-initiated reactions. The initial BrC_2H and 1,3-butadiene number densities are both 6.5×10^{13} cm^{-3} in a total gas density of 1.3×10^{17} cm^{-3}. Depletion of the BrC_2H signal at $t = 0$ when the laser fires is not apparent in the time profile for this species above the signal-to-noise ratio and therefore the percentage depletion of the radical precursor is estimated to be <1%. Fangtong et al. employed 193 nm BrC_2H photodissociation in a crossed-molecular beams experiment and indicated that approximately 6% of the BrC_2H is decomposed into Br + C_2H with a laser fluence of $\sim$400 mJ cm^{-2} [41]. The absorption of 248 nm light by BrC_2H is reported to be around 30 times lower than that of 200 nm light [42]. Due to the absence of absorption data at 193 nm, the assumption is made that the absorption at 193 nm is similar to 200 nm. Correcting for the laser fluence and different cross-section at 200 nm and 248 nm, an estimate of 0.035% for percentage of BrC_2H that photodissociates at 248 nm is calculated. Thus, an estimate for the number density of the C_2H radicals of $\sim 2 \times 10^{10}$ cm^{-3} is derived.

A portion of the gas escapes from the flow tube through a 650 μm diameter pinhole in the side of the tube into a chamber at a pressure of 10^{-5} Torr. The nearly effusive beam from this pinhole is skimmed by a 1.5 mm diameter skimmer before entering a differentially pumped ionization region. The gas beam is crossed by tunable synchrotron undulator vacuum ultraviolet (VUV) radiation that is dispersed by a 3 m monochromator (Chemical Dynamics Beamline at the Advanced Light Source of Lawrence Berkeley National Laboratory). The monochromatic VUV radiation energy is calibrated using known atomic resonances of Xe; at the conditions employed in these experiments the VUV light has a bandwidth of 20 meV. The VUV photon flux at each photon energy is measured using a calibrated photodiode (SXUV-100 International Radiation Detectors, Inc.). The masses of all cations formed in the ionization region are monitored with an orthogonal acceleration time-of-flight mass spectrometer equipped with a micro-channel plate detector. Mass spectra are taken at intervals of 20 μs, from −20 ms to 130 ms relative to photolysis. By additionally scanning the photon energy, time- and photon energy-resolved mass spectra are recorded, leading to a three-dimensional matrix of data consisting of ion intensity as a function of m/z (mass-to-charge ratio), reaction time, and photon energy.

The data can be examined in three ways: m/z *vs.* kinetic time, m/z *vs.* photon energy and photon energy *vs.* kinetic time. Photoionization spectra are constructed by integrating the data first over the desired m/z range and then over a suitable time window that corresponds to production of the species of interest in the reaction. Background contributions are removed by subtraction of the average pre-photolysis signal taken in the 20 ms before the photodissociation laser pulse. Finally, these background-subtracted signals are normalized for the VUV photon flux at each photon energy. Full time- and photon-energy-dependent spectra are collected three times to check for consistency, with 200 laser pulses at each VUV photon energy.

2.2. Bromoacetylene synthesis

The C_2H precursor in our experiment was bromoethyne (bromoacetylene, BrC_2H), which was synthesized according to the methodology of Bashford et al [43]. Synthesis was carried out in a triple-necked round-bottomed flask in a temperature-controlled water bath, connected to a water-cooled condensing column and a phosphorus pentoxide drying column. 10 g (50% w/w) sodium hydroxide solution was placed in the flask. The synthesis apparatus was purged of air using a helium flow and covered in aluminum foil to prevent any photolytic decomposition of the BrC_2H product. 15 g of 1,2-dibromoethylene and 18 ml of ethanol were injected into the flask. The flask was then heated to 85 °C for one hour, whilst maintaining a slow helium flow. Reaction products were collected in a liquid nitrogen cooled cold trap.

Purification of BrC_2H was carried out using three cold traps, covered in aluminum foil, attached in series and connected to a rotary pump, which attained a pressure of 100 m Torr. The temperatures of the three successive cold fingers were −65 °C, −115 °C and −196 °C. The impure product was pumped through the traps and was isolated in pure form at −115 °C and then allowed to sublime into a stainless steel cylinder with internal teflon coating. Helium was added to the cylinder to make a 5% mixture of BrC_2H; a dilute mixture is used to reduce the rate of degradation and polymerization.

The vapor pressure of BrC_2H was measured to be greater than 100 Torr at 298 K. A very high degradation rate is observed when exposed to light in solid state, and there is a high degradation rate at elevated temperatures, even in gaseous phase. Oxygen reacts extremely violently with BrC_2H and induces explosive polymerization [43]. The purity of the sample was checked with time-of-flight mass spectrometry using the multiplexed photoionization mass spectrometer (see Section 2.2) and the mass spectrum showed very little impurity.

2.3. Computational methodology

Identification of the isomers produced in the reaction relies on fitting the measured product photoionization spectra to known spectra of the pure compounds. In cases where these spectra have not been measured, due to the instability of the molecules, the spectra are simulated using computational methods. The photoionization spectrum of a molecule is computed by integrating the Franck–Condon factors between the vibrational modes of the ground and ionic states [44]. Employing the Gaussian 09 suite of programs [45], adiabatic ionization energies (AIEs) are calculated using the CBS-APNO or CBS-QB3 composite methods [46]. The geometries, harmonic vibrational modes and force constants for the molecules of interest are calculated at the B3LYP/cc-pVTZ level, and photoelectron spectra are simulated making use of the built-in Franck–Condon overlap feature of Gaussian 09 [47,48]. Note that this method is based on the assumption of direct ionization to the lowest-lying cationic state and does not describe autoionizing and shape resonances, dissociative ionization, and ionization to excited cationic states. Where applicable, the semiempirical method of Bobeldijk et al [49]. is used to estimate the absolute photoionization cross sections. Photoionization spectra used in the following analysis, simulated or experimental, are given in the Supporting Information.

Minima and first-order saddle points on the C_2H + 1,3-butadiene potential energy surface (PES) are explored using the M06-2X method [50] with a 6-31G* basis set, with energies calculated using the CBS-QB3 composite method [51,52]. The quantum-chemical calculations are performed using Gaussian 09 [45].

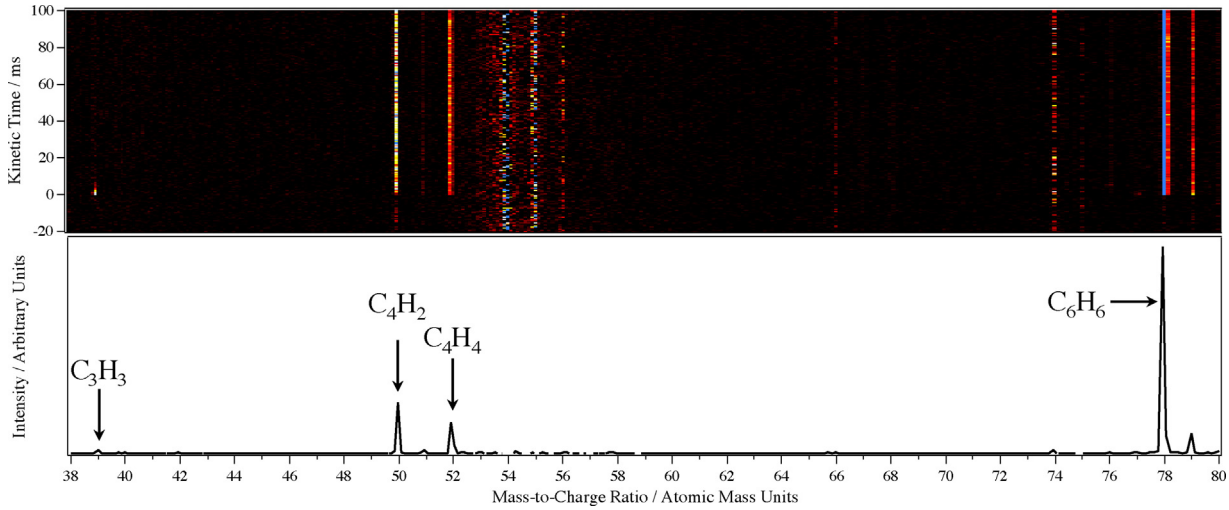

Fig. 1. Top panel is the background subtracted time-dependent mass spectrum integrated over the 8.2–11 eV photon energy range with the radical precursor BrC_2H and the closed-shell reactant 1,3-butadiene present in the flow tube. The products that are dependent on the photolysis laser pulse ($t = 0$) appear in the spectrum. Bottom panel shows a one-dimensional mass spectrum integrated over the 0–100 ms time range.

3. Results

3.1. Experimental results

C_2H + 1,3-butadiene reaction data were recorded over the 8.2–11.5 eV photon energy range, the −20–130 ms kinetic time range and up to 160 atomic mass units. Fig. 1 shows the background-subtracted product mass spectrum integrated over the 8.2–11 eV photon energy range as a function of kinetic time, along with the one-dimensional mass spectrum resulting from integration of the time-dependent spectrum over the 0–100 ms range. Four main peaks are present in the background subtracted mass spectrum, at m/z = 39, 50, 52 and 78, corresponding to molecular formulae C_3H_3, C_4H_2, C_4H_4 and C_6H_6, respectively. The peak at m/z = 79 is approximately 8% of the magnitude of the peak at m/z = 78, 6.1% of which is due to the presence of $^{12}C_5{}^{13}CH_6$ at the natural abundance. The remaining 1.9% is likely due to detection of C_6H_7, the reaction adduct, which may undergo radiative or collisional stabilization.

Mass spectra were also recorded at a single photon energy of 10.6 eV with only BrC_2H or only 1,3-butadiene in the flow. These data inform us of any direct photolysis products of the reactants, or secondary reactions involving these photolysis products that do not require both reactants entrained in the flow. One-dimensional mass spectra recorded with only BrC_2H or 1,3-butadiene entrained in the flow are given in the Supplementary Information and compared to a spectrum recorded when both reactants were entrained in the flow; these mass spectra are not background subtracted. When only BrC_2H is present in the flow, a peak at m/z = 50, due to detection of a species with molecular formula C_4H_2, is observed. When only 1,3-butadiene is present in the flow, four peaks appear in the spectrum: at m/z = 39, m/z = 50, m/z = 52 and m/z = 78 due to detection of species with the molecular formulae C_3H_3, C_4H_2, C_4H_4 and C_6H_6, respectively. The background subtracted temporal evolutions of these four signals, at m/z = 39, 50, 52 and 78, are examined and shown in Fig. 2. In Fig. 2, the solid black and dotted blue lines show the evolution of the signal when only BrC_2H and only 1,3-butadiene, respectively, are present in the flow and the dashed red line is the time profile of the signal when both reactants are present.

Fig. 2(a) shows that m/z = 39 is solely due to 1,3-butadiene photolysis. The depletion rate of the m/z = 39 concentration when both reactants are present (dashed red line) is faster due to the fact that there are more species in the flow that can react with the radical. The peak at m/z = 50 is predominantly due to photolysis of BrC_2H, with a very small contribution from 1,3-butadiene photolysis, Fig. 2(b). The component of the m/z = 50 signal that is due to 1,3-butadiene photolysis has a slower rise time than that for the total signal when both reactants are present and the signal is due to BrC_2H photolysis. This slower rise time suggests that the source of this species is a secondary reaction rather than primary photolysis of 1,3-butadiene. Fig. 2(c) shows that the peak at m/z = 52 is primarily due to photolysis of 1,3-butadiene, yet the concentration of this species increases when both reactants are entrained in the flow. The relative areas of the peaks at m/z = 52 with only 1,3-butadiene in the flow and with both reactants in the flow reveal that approximately 73% of the products at this mass arise from photolysis of 1,3-butadiene. Possible sources of the remaining 27%, which arises only when both reactants are present, will be discussed later. The time profiles for m/z = 78 shown in Fig. 2(d) reveal that the majority of the signal, approximately 90%, only appears when both reactants are present in the flow. When only 1,3-butadiene is present, a small signal appears at m/z = 78 that has a very slow rise time that accounts for no more than 10% of the total when both reactants are present. This signal is likely due to the recombination of C_3H_3 radicals (m/z = 39) that are formed by 1,3-butadiene photolysis, a process that has been observed before [53], or a reaction of C_3H_3 with 1,3-butadiene. Nevertheless, it is clear that formation of C_6H_6 (m/z = 78) is the predominant reaction channel in the C_2H + 1,3-butadiene reaction.

The peak at m/z = 50 has been identified by its photoionization spectrum as 1,3-butadiyne [54] (C_4H_2), Fig. 3(a). Upon photolysis of BrC_2H, 1,3-butadiyne forms by reaction of the photolytically produced C_2H radical with the radical precursor *via* the mechanism outlined in Scheme 1 in Fig. 4 [55]. The peaks at m/z = 39 and 52 have been identified as propargyl radicals [56] (C_3H_3), Fig. 3(b), and vinyl acetylene [54] (C_4H_4), Fig. 3(c), respectively. Few studies have dealt with the fate of 1,3-butadiene following excitation at 248 nm. However, numerous studies explored the excitation and photolysis of 1,3-butadiene in the 193–220 nm range, from which it is found that the primary dissociative channel leads to formation of $C_3H_3 + CH_3$ [14,57–60]. In addition to $C_3H_3 + CH_3$, the following minor photolysis channels have also been reported in the 193–220 nm energy range: $C_4H_5 + H$, $C_4H_4 + H_2$, $C_2H_3 + C_2H_3$ and $C_2H_2 + C_2H_4$ with varying relative ratios [14,59,60]. The 1,3-butadiene cross-section for absorption at 248 nm is nearly two orders of

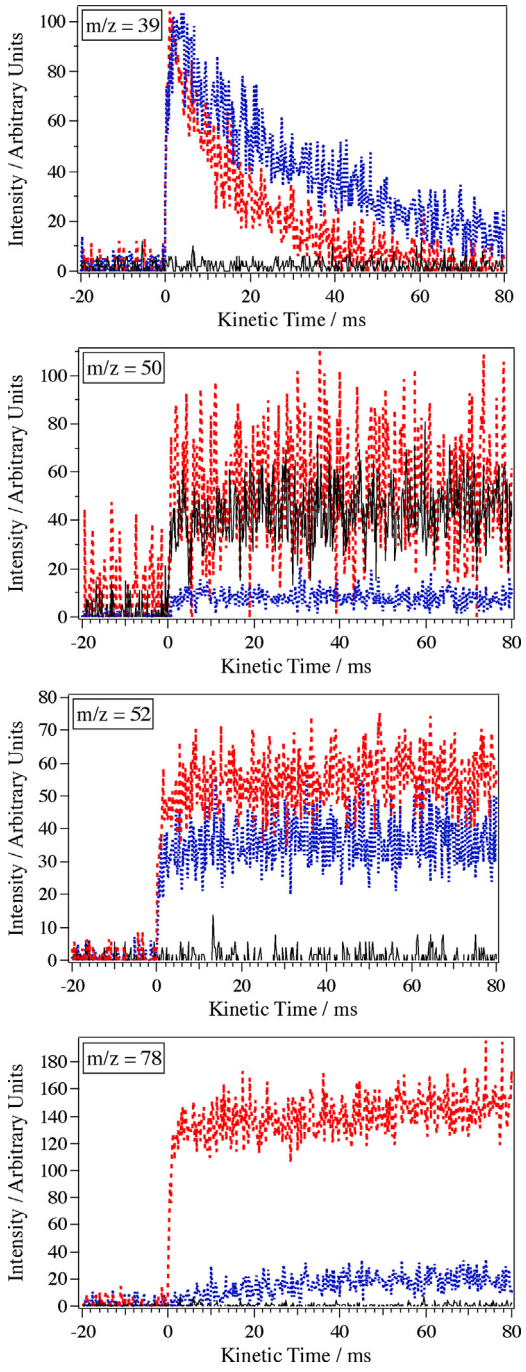

Fig. 2. Background subtracted time profiles for $m/z = 39$, 50, 52 and 78 with only BrC_2H and He in the flow (solid black line), with only 1,3-butadiene and He in the flow (dotted blue line) and with both BrC_2H and 1,3-butadiene (and He) in the flow (dashed red line). (For interpretation of the references to colour in this figure legend, the reader is referred to the web version of this article.)

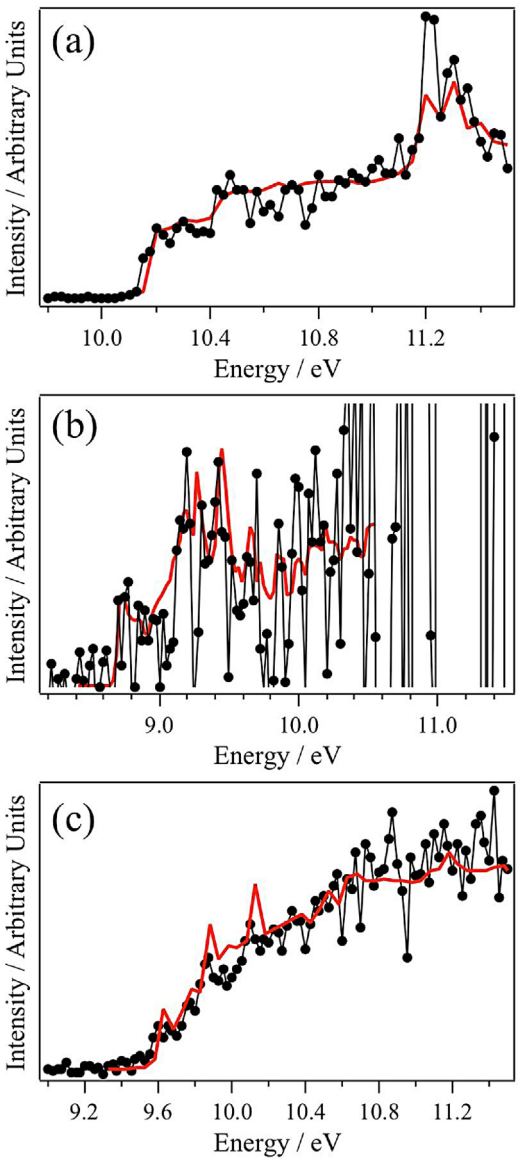

Fig. 3. Photoionization spectra of the species detected at (a) $m/z = 50$, (b) $m/z = 39$ and (c) $m/z = 52$. The red solid lines show the photoionization spectra of (a) 1,3-butadiyne, (b) propargyl and (c) vinyl acetylene. (For interpretation of the references to colour in this figure legend, the reader is referred to the web version of this article.)

magnitude smaller than at 193 nm and certain channels are energetically inhibited, such as formation of two vinyl radicals (C_2H_3) by cleavage of the central C—C bond. It has been shown that in the 220–260 nm range, photolysis of 1,3-butadiene leads to formation of CH_3 radicals (in conjunction with C_3H_3) with a branching of 75% [61]. Propargyl radicals are formed in conjunction with CH_3 (Scheme 2 in Fig. 4), although methyl is not detected in our experiment. The absence of CH_3 signal is likely due to the fact that the photoionization cross-section of CH_3 is much smaller than that of propargyl radicals; at 10.413 eV, for example, it is around 4 times lower [56]. In addition, the mass discrimination factor of the mass-spectrometer means detection of species with $m/z = 39$ is nearly twice as likely as species with $m/z = 15$ [56]. The majority of the signal at $m/z = 52$, vinyl acetylene, is due to 1,3-butadiene photolysis, Scheme 3 in Fig. 4, or secondary reactions of photolysis products, but a small additional amount is due to the presence of both BrC_2H and 1,3-butadiene in the flow. Vinyl acetylene could potentially be a product of C_2H + 1,3-butadiene reaction *via* a mechanism of addition and β-C—C bond scission to yield vinyl acetylene + C_2H_3, Scheme 4 in Fig. 4. However, vinyl radicals ($m/z = 27$) are not observed above the background level in the mass spectra, perhaps because they rapidly dissociate or react.

The current experiment shows the predominant channel in the C_2H + 1,3-butadiene reaction to be addition of the radical to one of the unsaturated carbon sites of 1,3-butadiene followed by H-loss to give C_6H_6. The fact that the amount of vinyl acetylene ($m/z = 52$) detected increases by 27% when both BrC_2H and 1,3-butadiene are present in the flow suggests that a pathway to vinyl acetylene

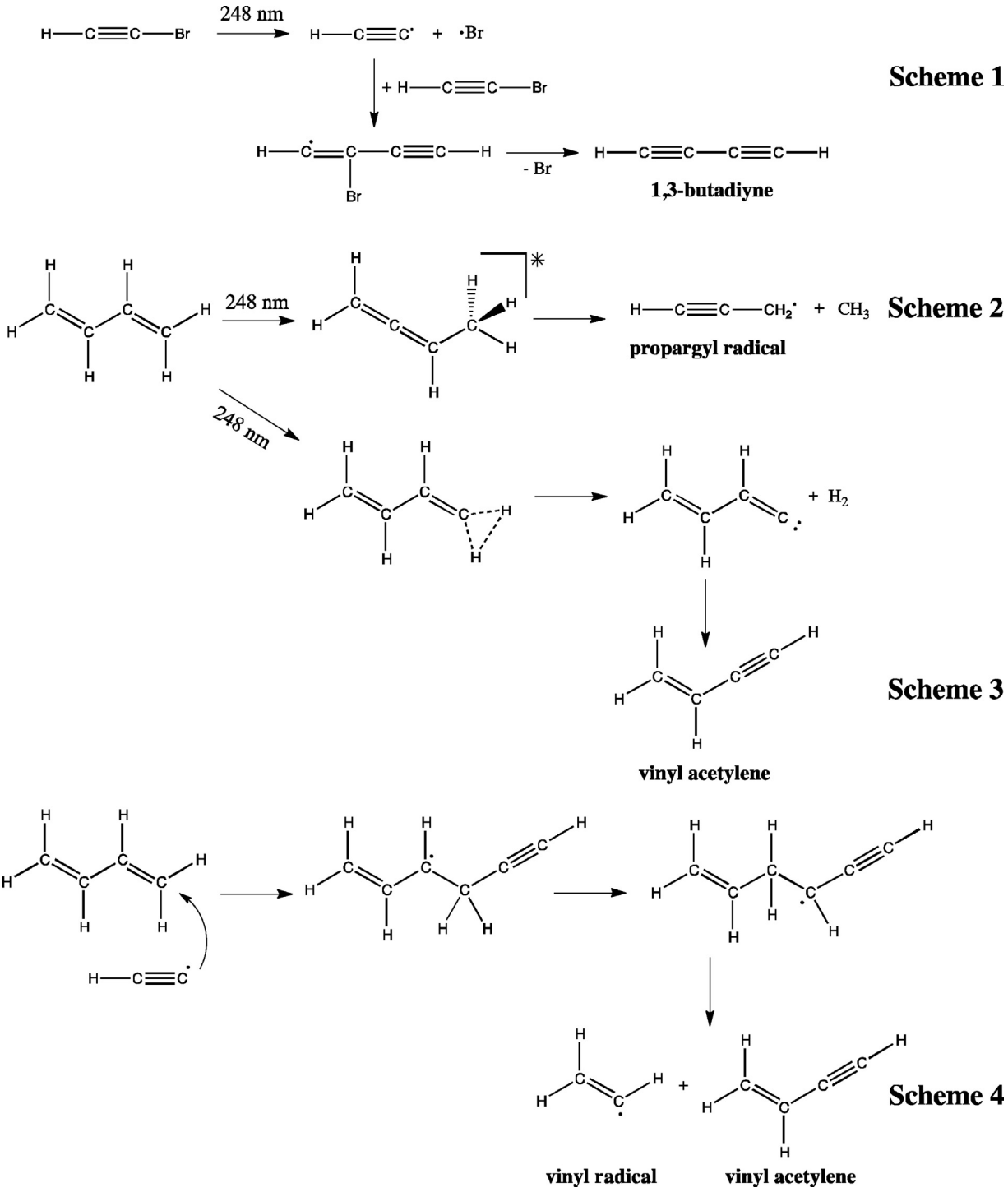

Fig. 4. Scheme 1: Reaction mechanism for formation of 1,3-butadiyne *via* photolysis of BrC_2H at 248 nm to give C_2H + Br, followed by reaction of the C_2H with BrC_2H and Br elimination. Photolysis of 1,3-butadiene by 248 nm light to give $C_3H_3 + CH_3$ (Scheme 2) and vinyl acetylene + H_2 (Scheme 3). Scheme 4: Possible reaction mechanism for production of vinyl acetylene + vinyl radicals from the reaction of C_2H with 1,3-butadiene.

(C_4H_4) + vinyl radicals (C_2H_3) may also represent a small fraction of the reactivity. In addition, the peak at $m/z = 79$ has an area that is 31% larger than expected from $^{12}C_5{}^{13}CH_6$ alone, suggesting that some reactive intermediates are stabilized radiatively or by collisions. Based solely on the peak areas of these respective signals, and not accounting for the absolute photoionization cross-sections of the constituent species, the process that results in $m/z = 78$ accounts for 96% of reactivity, that resulting in vinyl acetylene ($m/z = 52$) accounts for 4% and the proportion of intermediates that are stabilized is 0.2%. To identify isomers formed, the measured photoionization spectrum of the products at $m/z = 78$ is examined. As shown earlier, there is a contribution to the peak at $m/z = 78$ when only 1,3-butadiene is present in the flow, arising from C_3H_3 recombination. This C_3H_3 recombination accounts for less than 10% of the total signal at $m/z = 78$ when both reactants are present in the flow. The photoionization spectrum of the C_6H_6 products from C_3H_3 recombination [62] has a significantly different shape than that of the $m/z = 78$

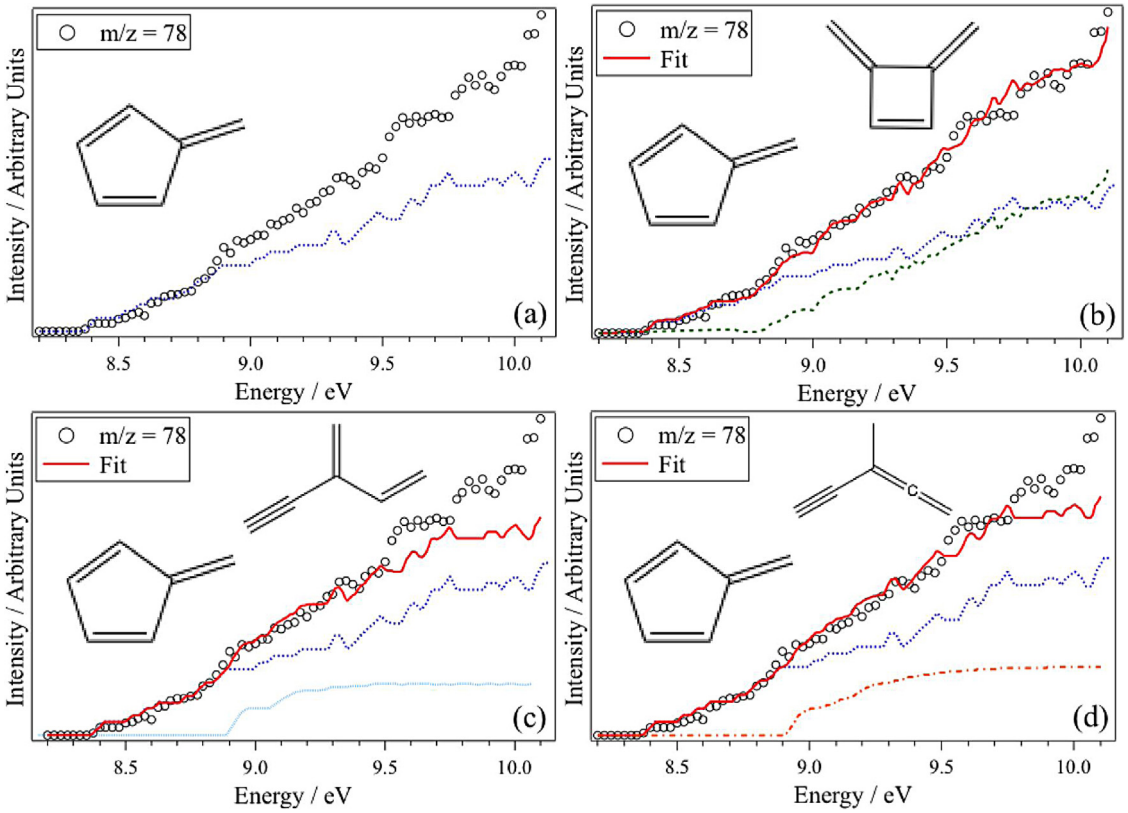

Fig. 5. Black open circles show the measured photoionization spectrum for the products of the C_2H + 1,3-butadiene reaction at m/z = 78. The dark blue dotted line shows the photoionization spectrum for fulvene, which fits the measured spectrum up to a photon energy of 8.85 eV, as shown in (a). In (b), the dashed green line shows the experimental photoionization spectrum of 3,4-dimethylenecyclobut-1-ene and the solid red line shows the fit to the data, constructed by adding weighted contributions of the fulvene and 3,4-dimethylenecyclobut-1-ene spectra. The fit in (c), shown by the solid red line, is constructed by adding a contribution of 3-methylene-1-penten-4-yne, the photoionization spectrum shown by the pale blue line, to the fulvene component. The fit in (d), shown by the solid red line, is constructed by adding a contribution of 3-methyl-1,2-pentadien-4-yne, the photoionization spectrum shown by the orange dot-dashed line, to the fulvene component. (For interpretation of the references to colour in this figure legend, the reader is referred to the web version of this article.)

products observed in this experiment. Correcting the spectrum for the products of the C_2H + 1,3-butadiene reaction for the 10% contribution from C_3H_3 recombination has a negligible effect on the shape of the measured spectrum. Nevertheless, this corrected spectrum is used in the following analysis. The onset of the measured photoionization spectrum of the products of C_2H + 1,3-butadiene with m/z = 78 is at 8.36 eV, which matches exactly with the ionization onset of fulvene [63]. Indeed, the measured photoionization spectrum can be reproduced by the experimentally measured photoionization spectrum of fulvene [36] up to a photon energy of ≈8.85 eV, Fig. 5(a). From the deviation of the measured signal from the fulvene photoionization spectrum above 8.85 eV, it is evident that additional isomers must contribute to the overall signal. There are three isomers of C_6H_6 that have ionization onsets in the 8.85 eV region; these are 3,4-dimethylenecyclobut-1-ene (8.8 eV [63]), 3-methylene-1-penten-4-yne (no experimental value available, calculated in this work using the CBS-APNO methodology to be 8.89 eV [64]) and 3-methyl-1,2-pentadien-4-yne (no experimental value available, calculated in this work using the CBS-APNO methodology to be 8.90 eV [64]). It seems likely that one or more of these isomers is formed.

A good fit to the measured photoionization spectrum can be obtained with a weighted contribution of the experimentally measured photoionization spectra of fulvene [36] and 3,4-dimethylenecyclobut-1-ene [36], as shown in Fig. 5(b). Adjusting the scaling factors for the absolute photoionization cross-sections of these two isomers yields branching ratios of 51% fulvene and 49% dimethylenecyclobut-1-ene. Alternatively, if a contribution from 3-methylene-1-penten-4-yne is included in addition to fulvene, as shown in Fig. 5(c), a good fit of the measured spectrum can be obtained up to a photon energy of around 9.5 eV. The photoionization spectrum of 3-methylene-1-penten-4-yne has not been measured experimentally and so a simulated spectrum reported by Soorkia et al. [36] is used in the current analysis. These simulations often reproduce the experimental spectra for the transition from the ground electronic state of the neutral to the ground electronic state of the cation. However, excited electronic states of the cation and autoionization are not considered in the calculation and so the simulated spectrum may not have the same shape as the real spectrum at higher photon energies. For this reason it is difficult to determine whether the deviation of the fit from the measured spectrum in Fig. 5(c) at 9.5 eV is due to formation of other isomers with higher ionization energies or due to photo-excitation to excited electronic states of 3-methylene-1-penten-4-yne. Finally, a good fit to the measured spectrum can also be obtained if a contribution of 3-methyl-1,2-pentadien-4-yne is included, in addition to the fulvene component, Fig. 5(d). An experimental photoionization spectrum of 3-methyl-1,2-pentadien-4-yne is not available and so was simulated using the methodology outlined in the Experimental section. Using fulvene and 3-methyl-1,2-pentadien-4-yne, the fit begins to deviate from the data at around 9.75 eV, which could be due to excited electronic states of the 3-methyl-1,2-pentadien-4-yne cation or additional isomers being formed.

Benzene has vertical ionization energy of 9.244 eV [63]. There is not a distinct rise in the measured photoionization spectrum at 9.244 eV, thus, it seems that benzene is not a major product of the title reaction. 1,3-hexadien-5-yne has an ionization energy of

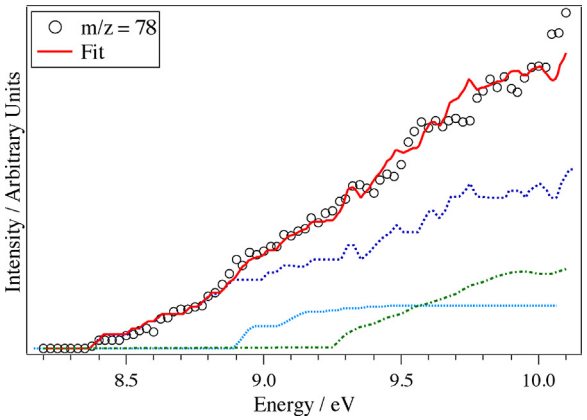

Fig. 6. Black open circles show the measured photoionization spectrum of the C_6H_6 products of the C_2H + 1,3-butadiene reaction at 4 Torr and 298 K. Dark blue dashed line shows the experimental photoionization spectrum of fulvene. Pale blue dotted line shows the simulated photoionization spectrum of 3-methylene-1-penten-4-yne. Green dot-dashed line shows the experimental photoionization spectrum of benzene. The solid red line shows a fit to the data constructed using an appropriately weighted sum of each of these calibration photoionization spectra (dark blue, pale blue and green lines). (For interpretation of the references to colour in this figure legend, the reader is referred to the web version of this article.)

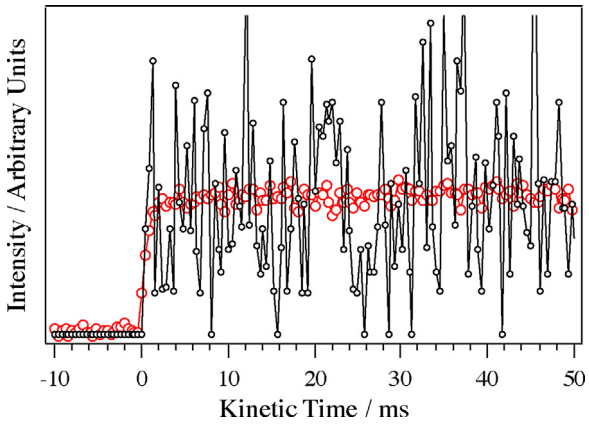

Fig. 7. Large red circles show the time profile of the C_6H_6 product integrated over the 8.2–10.5 eV range. Small black circles show the time profile of the fulvene product, which is obtained by integrating over the 8.2–8.6 eV range. Although the signal-to-noise of the fulvene-only signal is low, the risetime is consistent with that of the sum of all C_6H_6 isomers and is inconsistent with contributions from H-atom assisted isomerization. The laser fires at $t = 0$. (For interpretation of the references to colour in this figure legend, the reader is referred to the web version of this article.)

9.2 eV [63], very close to that of benzene. Reasonable fits to the measured photoionization spectrum can be made with weighted contributions of both of these isomers, but only benzene will be discussed further, given its significance in combustion and astrochemical environments. However, since two possible combinations of isomers can reproduce the data, the maximum branching fraction extracted is for a sum of benzene and 1,3-hexadien-5-yne. As shown in Fig. 6, a fit to the measured spectrum can be obtained with a combination of the experimental PI spectrum of fulvene [36], the simulated spectrum of 3-methylene-1-penten-4-yne and the experimental PI spectrum of benzene [54]. The scaling factors for each PI curve that give the best fit to the data are adjusted for the absolute photoionization cross-section of each species, yielding a maximum possible branching for the sum of benzene and 1,3-hexadien-5-yne.

It is clear from the product photoionization spectrum that the dominant product of the C_2H + 1,3-butadiene reaction is fulvene. The identity of the other isomers formed includes one or a combination of 3,4-dimethylenecyclobut-1-ene, 3-methylene-1-penten-4-yne and 3-methyl-1,2-pentadien-4-yne. Using the experimental or simulated photoionization spectra available at this time, the measured product PI spectrum can be reproduced by the sum of the PI spectra of each isomer multiplied by a scaling factor. The scaling factors need to be adjusted for the absolute photoionization cross-section of each isomer. An uncertainty of 50% is estimated for the cross-sections calculated using the semi-empirical method of Bobeldjik et al. [49], and an uncertainty of 20% is estimated for the absolute cross-section of benzene, which has been experimentally measured. Adjusting the scaling factors for the absolute photoionization cross-section of each isomer, a branching fraction for the fulvene product with an associated error and maximum possible branching fractions for 3,4-dimethylene-cyclobut-1-ene, 3-methylene-1-penten-4-yne and 3-methyl-1,2-pentadien-4-yne are calculated and given in Table 1. Also shown in Table 1 is the maximum possible branching fraction for the sum of benzene and 1,3-hexadien-5-yne, given the significance of the benzene molecule in a variety of environments. The ground state reaction exothermicities for formation of each proposed isomer + H from C_2H + 1,3-butadiene, calculated at the CBS-QB3 level of theory, are also given in Table 1.

The results strongly indicate that under the conditions of this experiment (4 Torr and 298 K), fulvene has a branching fraction of (57 ± 30)%. The maximum branching fractions for the other

Table 1
Branching fraction for fulvene and upper limits for the branching fractions for 3,4-dimethylenecyclobut-1-ene, 3-methylene-1-penten-4-yne, 3-methyl-1,2-pentadien-4-yne and the sum of benzene and 1,3-hexadien-5-yne derived from fitting the measured photoionization spectrum of $m/z = 78$ in the reaction of C_2H + 1,3-butadiene. Also given are the CBS-QB3 ground state reaction exothermicities for forming the specific product isomer + H from C_2H + 1,3-butadiene.

Product isomer	Branching fraction/%	Reaction exothermicity (including H atom co-product)[a]/kJ mol^{-1}
Fulvene	57 ± 30	−247
3,4-Dimethylenecyclobut-1-ene	<74	−123
3-Methylene-1-penten-4-yne	<24	−101
3-Methyl-1,2-pentadien-4-yne	<31	−59
Benzene	<45	−384
1,3-Hexadien-5-yne		−116

[a] All reaction exothermicities are ground state and calculated at the CBS-QB3 level of theory.

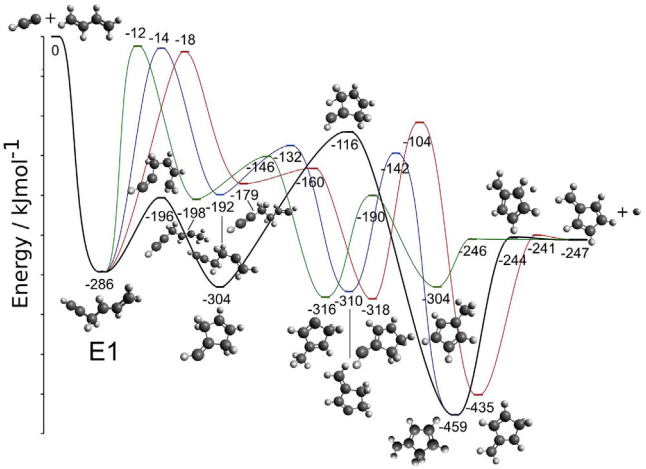

Fig. 8. Schematic of the potential energy profile showing the enthalpy *vs* reaction coordinate, illustrating four possible reaction pathways to fulvene formation in the C_2H + 1,3-butadiene reaction.

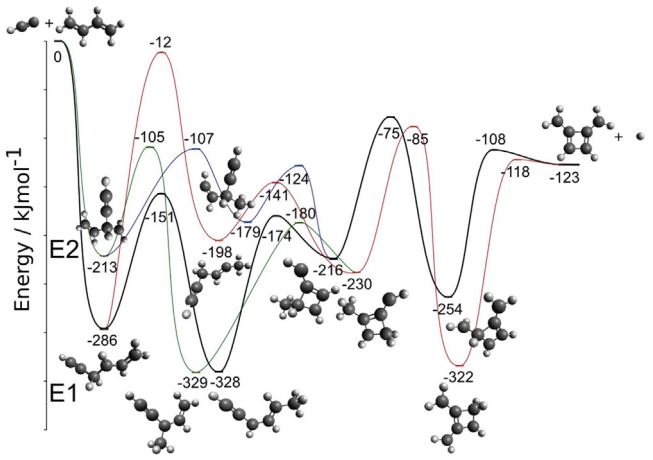

Fig. 9. Schematic of the potential energy profile showing the enthalpy *vs* reaction coordinate, illustrating four possible reaction pathways to 3,4-dimethylenecyclobut-1-ene formation in the C_2H + 1,3-butadiene reaction.

possible cyclic isomers, 3,4-dimethylenecyclobut-1-ene and benzene, are estimated to be 74% and 45%, respectively. What is intriguing about these values is that the branching fraction for fulvene and the maxima for 3,4-dimethylenecyclobut-1-ene and benzene are significant, and could potentially account for nearly all products formed, suggesting that cyclization reactions can compete favorably with direct H-loss to give straight-chain isomers. The reaction of C_2H + 1,3-butadiene may be a significant source of cyclic molecules in combustion and astrochemical environments.

Since the reactions take place in a collisional environment, it is necessary to verify that collisions with species other than He in the flow do not alter the product distribution. To verify that H-assisted isomerization, or any other secondary process, does not change the isomer distribution, the signal rise time of the fulvene product is compared to the signal rise time for the m/z = 78 peak at all photon energies. By integrating the data over the 8.2–8.6 eV photon energy range the temporal behavior of the fulvene component can be examined without contribution from other product isomers. It is found that the rise time of the fulvene product after the laser pulse is the same as the rise time for the peak as a whole, Fig. 7, confirming that fulvene formation is not a result of H-assisted isomerization from another product, at least not on the millisecond time scale. The initial C_2H concentration (and hence the H-atom and C_6H_6 concentrations) is estimated to be 2×10^{10} cm^{-3}, so the characteristic time for H-atom assisted isomerization even for an unrealistically large rate coefficient of 10^{-9} cm^3 s^{-1} would be in excess of 50 ms. In addition, the photoionization spectrum was examined in 5 ms intervals over the 0–100 ms kinetic time range; the shape of the spectrum, and therefore the isomer distribution, remained the same over the entire range. Another point to address is the possibility of unimolecular isomerization of the C_6H_6 product. Isomerization of the closed-shell products formed by the H-loss involves prohibitively high energetic barriers and does not occur in the current experiment at 298 K.

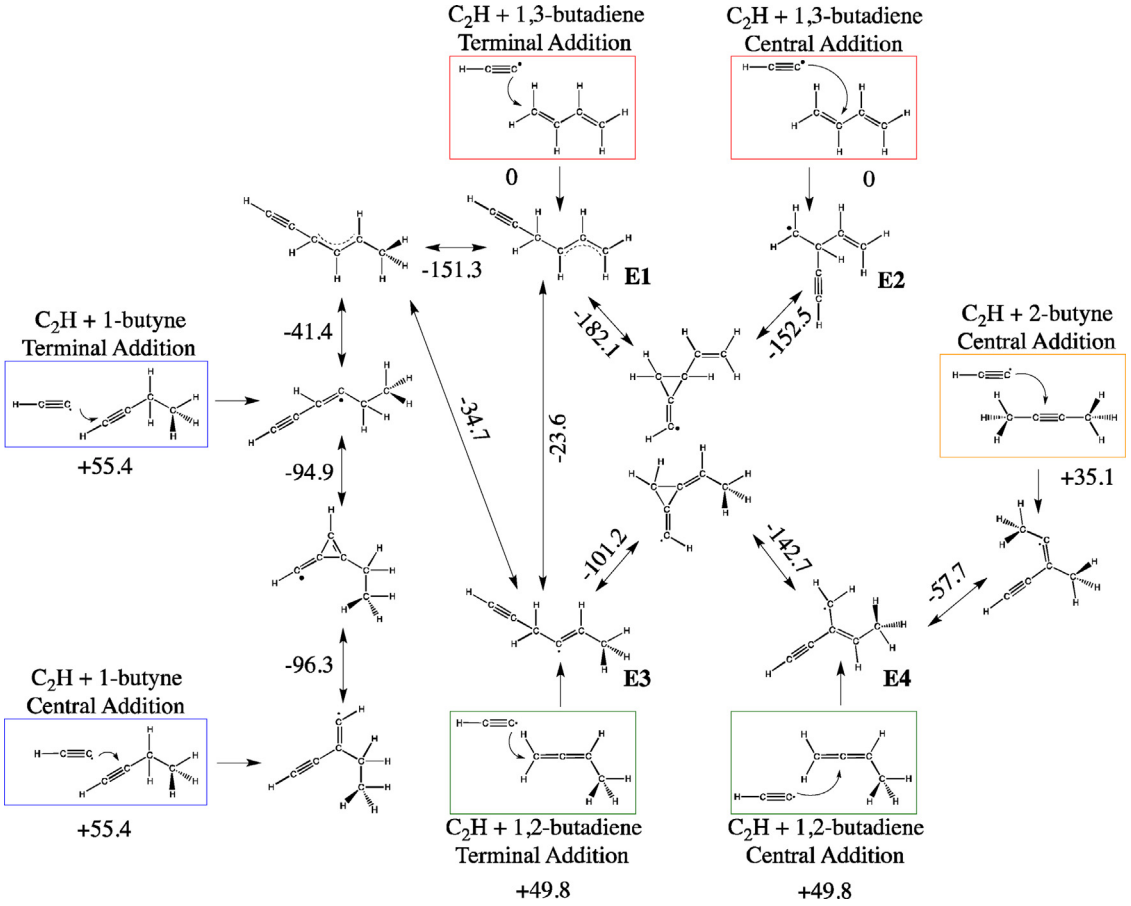

Fig. 10. Schematic of the addition reactions of C_2H on the unsaturated sites of 1,3-butadiene, 1,2-butadiene, 1-butyne and 2-butyne. The most facile inter-conversions between the initial adducts are shown. Transition state energies relative to the infinitely separated C_2H and 1,3-butadiene reactants are in kJ mol^{-1}. Also given are the energies of the infinitely separated C_2H and 1,2-butadiene, 1-butyne and 2-butyne relative to the infinitely separated C_2H and 1,3-butadiene in kJ mol^{-1}.

3.2. Computational results

A quantum chemical investigation of possible reaction mechanisms resulting in fulvene and 3,4-dimethylenecyclobut-1-ene was carried out. The principal aim of the quantum chemical calculations is to uncover reaction pathways to fulvene and 3,4-dimethylenecyclobut-1-ene formation that may be able to compete with the pathways to 1,3-hexadien-5-yne and benzene formation outlined by Jones et al. Structures of stationary points and transition states were determined at the M06-2X/6-31G* level and energies computed using the CBS-QB3 composite method. These calculations do not attempt to predict the products of the title reaction quantitatively, but they do provide auxiliary information to the experimental results obtained. Four energetically possible pathways to fulvene formation and four pathways to 3,4-dimethylenecyclobut-1-ene formation in the C_2H + 1,3-butadiene reaction were found. Schematics of the energy profile of these pathways as a function of the reaction coordinate are given in Figs. 8 and 9.

C_2H can add to either the terminal or central unsaturated carbon atoms of 1,3-butadiene, leading to two structurally different encounter complexes, termed E1 and E2, respectively. E1 and E2 have energies of $-286\,kJ\,mol^{-1}$ and $-213\,kJ\,mol^{-1}$ relative to the asymptote for the infinitely separated reactants. Transformation of E1 to E2 and vice versa can occur *via* a 3-membered-ring isomer, as shown schematically in Fig. 10. In addition, E1 could directly lose an H atom to yield 1,3-hexadien-5-yne or 1,2-hexadien-5-yne and E2 could lose an H atom to yield 3-methylene-1-penten-4-yne. Alternatively, isomerization of E1 or E2 *via* H-shifts or cyclization could occur. The simplest pathway to fulvene formation that was found involves cyclization of E1 *via* a low barrier that is $90\,kJ\,mol^{-1}$ above the energy of E1, a single H-shift and H-loss to yield fulvene + H, denoted by the thick black line in Fig. 8. Three other possible fulvene-formation pathways were also determined that involve isomerization of E1 *via* H-shift as their first step; these pathways are denoted by the green, blue and red curves in Fig. 8 and correspond to 2,1-, 2,3- and 1,3-H-shifts, respectively. These three alternate pathways involve an additional H-shift step *via* transition states that lie high in energy compared to E1 and also to the barriers involved in the first pathway described. Consequently, it seems very likely that the simplest pathway, involving cyclization prior to H-shift, would be more likely to account for the fulvene formation in the C_2H + 1,3-butadiene reaction than the pathways involving H-shift prior to cyclization.

Four energetically possible reaction pathways to 3,4-dimethylenecyclobutene-formation were also found, two from addition of the C_2H radical to the terminal carbon atom and two from addition of the radical to the central carbon atom of 1,3-butadiene, Fig. 9. All routes to 3,4-dimethylenecyclobutene that have been calculated involve a primary H-shift isomerization of E1 or E2 followed by cyclization, a secondary H-shift and finally H-loss. E1 can undergo 4,1- or 2,1-H-shift to yield straight-chain radicals that can undergo cyclization reactions to give the 4-membered ring backbone of 3,4-dimethylenecyclobut-1-ene. The cyclic intermediate then undergoes a secondary H-shift, followed by H-loss. The 2,1-H-shift has a very high barrier, lying only $12\,kJ\,mol^{-1}$ below the energy of the separated reactants and so it is postulated that this route is unlikely to play an important role in 3,4-dimethylenecyclobut-1-ene formation compared to the pathway that involves 4,1-H-shift. E2 could isomerize *via* a shift of the H that was originally bound to the central carbon atom on which the radical addition took place to the neighboring terminal position. Alternatively, one of the H atoms bound to the terminal carbon furthest from the site of radical addition could shift to the opposite terminal position. The radicals resulting from these H-shifts could then undergo a cyclization isomerization and a secondary H-shift, followed by H-loss.

4. Discussion

To understand the experimental results obtained in this study of the C_2H + 1,3-butadiene reaction, it is helpful to put them in the context of the PES considering multiple C_4H_6 isomers. Despite the fact that the isomeric form of the reactant C_4H_6 dictates where the C_6H_7 surface is accessed, which may influence the product distributions, these starting points are inherently connected, as illustrated in Fig. 10. Only the simplest inter-conversions (fewest steps) between the primary adducts are given in Fig. 10, although others exist. CBS-QB3 energies for each transition state involved in the transformations shown in Fig. 10 have been calculated relative to the C_2H + 1,3-butadiene ground state asymptote. Conversion of the initial adduct of terminal addition of C_2H on 1,3-butadiene (E1) to the initial adduct of terminal addition on 1,2-butadiene (E3) occurs *via* a single H-shift with a transition state that lies $23.6\,kJ\,mol^{-1}$ below the asymptote for the separated C_2H + 1,3-butadiene reactants. The dominant products of the C_2H + 1,2-butadiene reaction are predicted by Jamal et al. to be 3-methylene-1-penten-4-yne + H [20]. However, CH_3-loss is also predicted by Jamal et al. to occur in the C_2H + 1,2-butadiene reaction, giving isomers of C_5H_4 with a branching fraction between 9 and 16% of the reactivity [20]. The fact that C_5H_4 is not detected above the signal-to-noise ratio in the current experimental study of the C_2H + 1,3-butadiene reaction implies that the inter-conversion *via* a H-shift from the initial adduct of the C_2H + 1,3-butadiene terminal addition to the initial adduct of the C_2H + 1,2-butadiene terminal addition is unfavorable. Conversion of E1 and E2 to the initial adducts of the C_2H + 1-butyne or 2-butyne reactions involves at least two H-shifts and so one might expect these conversions to be less favorable than to the initial adducts of the C_2H + 1,2-butadiene reaction. Indeed, the C_2H + 2-butyne and C_2H + 1-butyne reactions are predicted by Jamal et al. to yield high branching fractions of C_5H_4 isomers [26], and the experimental study of the C_2H + 1-butyne reaction by Soorkia et al. found a branching of 56% for C_5H_4 [36], whereas no C_5H_4 isomers are detected in this study. In summary, it seems that E1 and E2 do not isomerize to explore the areas of the C_6H_7 PES accessed in the C_2H + 1,2-butadiene, 1-butyne and 2-butyne reactions. These insights indicate that isomerizations of the adducts E1 and E2 *via* H-shift are not favorable under the current conditions.

Mebel and co-workers have published *ab initio* investigations of the C_2H reaction with all non-cyclic isomers of C_4H_6 (1,3-butadiene, 1,2-butadiene, 1-butyne and 2-butyne) [20,23,26]. All of the branching ratios reported in each of those papers are given in Table 2. The experimentally obtained branching fractions in the C_2H + 1-butyne reaction reported by Soorkia et al. [36], are also given in Table 2. The results of Soorkia et al. were obtained by employing the same experimental apparatus as in the present study. The branching fractions for the C_2H + 1-butyne reaction reported by Soorkia et al [36]. are significantly different from the *ab initio* results of Jamal et al [26]. In another computational study by Mandal et al. [65], the experimental findings of Soorkia et al. are corroborated and reaction pathways to each detected isomer are found. Unfortunately, overall branching fractions are not given in the publication of Mandal et al.

The experimentally derived branching ratios in the C_2H + 1,3-butadiene reaction presented here, particularly the high branching fraction for fulvene, are not in agreement with the experimental and computational results published by Jones et al [23]. Some possible reasons for these disagreements are discussed here, and, clearly, there are still unanswered questions in C_2H + C_4H_6 reaction systems that merit further investigation. Firstly, the branching

Table 2
Previously published experimental and theoretical branching fractions for the products of C_2H reactions with 1,3-butadiene, 1,2-butadiene, 1-butyne and 2-butyne.

Product channel	C_2H + 1,3-butadiene [23] (experiment and theory, Jones et al.)	C_2H + 1,2-butadiene [20] (theory, Jamal et al.)	C_2H + 2-butyne [26] (theory, Jamal et al.)	C_2H + 1-butyne [26] (theory, Jamal et al.)	C_2H + 1-butyne [36][f] (experiment, Soorkia et al.)
Benzene + H	40[a]-20[b],30[b,c]	0	0[e]	0[e]	<10
1,3-Hexadien-5-yne + H	60[a]-80[b], 70[b,c]	0	0	3.6[a]-2.4[d]	–
3-Methylene-1-penten-4-yne + H	0[e]	90.8[a]-83.68[d]	0.4[a]-0.5[d]	57[a]-36[d]	2.4
Penta-1,4-diyne + CH_3	0[e]	6.98[a]-11.86[d]	98.6[a]-97.7[d]	0[e]	–
1,2-Pentadien-4-yne + CH_3	0[e]	1.78[a]-3.38[d]	0	32.9[a]-42.6[d]	56
1,4-Hexadiyne + H	0[e]	0.10[a]-0.26[d]	0[e]	0[e]	–
3-Methyl-1,4-pentadiyne + H	0[e]	0.06[a]-0.32[d]	0[e]	0[e]	–
Diacetylene + C_2H_5	0[e]	0.12[a]-0.18[d]	0	4.2[a]-15.5[d]	–
2,3-Hexadien-5-yne + H	0[e]	0.04[a]-0.1[d]	0	1.3[a]-1.2[d]	8.4
3-Methyl-1,2-pentadien-4-yne + H	0[e]	0.02[a]-0.08[d]	1.0[a]-1.7[d]	0	–
1,3-Hexadiyne + H	0[e]	0	0	0.9[a]-1.8[d]	4.2
Methyldiacetylene + CH_3	0[e]	0[e]	0[e]	0.03[a]-0.2[d]	14
Fulvene + H	0[e]	0[e]	0	0	5.4
3,4-Dimethylenecyclobut-1-ene + H	0[e]	0[e]	0	0	9.6
1,2,3,4-Hexatetraene + H	0[e]	0	0[e]	0[e]	–
1,2-Hexadien-5-yne + H	0[e]	0	0[e]	0[e]	–
1,2-Hexadien-4-yne + H	0[e]	0	0[e]	0[e]	–

[a] At zero collision energy.
[b] At 45 kJ mol^{-1} collision energy.
[c] Experimental value.
[d] At 29 kJ mol^{-1} collision energy.
[e] Not specified so assumed to be zero.
[f] Calculated from the relative m/z = 64:m/z = 78 peak areas in Ref. [36] and corrected for the isomeric composition of each peak and the estimated photoionization cross-section of each isomer that are reported in the paper.

fractions of (70 ± 10)% and (30 ± 10)% for 1,3-hexadien-5-yne and benzene, respectively, in the C_2H + 1,3-butadiene reaction reported by Jones et al [23]. were obtained employing a crossed-molecular-beams technique. In this technique the reaction between the radical and reactant takes place in a single-collision environment at elevated collision energy. Although their collision energy of 45 kJ mol^{-1}, translates to a thermal energy of 5400 K, the excess energy is likely rapidly randomized within the initial C_6H_7 reactive complex. In contrast, in the current study the reactions take place in a collisional environment and at 298 K. Excess translational or internal energy of the C_2H reactant is collisionally relaxed prior to reaction with 1,3-butadiene, and collisional redistribution of energy in the C_6H_7 complex is also possible. The distribution of angular momentum states in the C_6H_7 may also be substantially different in the two experiments. In the crossed-molecular beams investigation of Jones et al., products are ionized *via* electron impact at 80 eV, the angularly resolved TOF spectra are recorded and a product translational energy distribution in the center-of-mass frame is calculated. The identification of the isomers is carried out by fitting the experimental data to modeled distributions that are obtained by forward convolution. The molecular beam experiments are particularly selective for benzene, the most exothermic channel, because it can appear at energies that are closed for other reaction products. The identification of isomers in the present study is spectroscopic, and the identification of fulvene by its photoionization spectrum is independent of the energy disposal in the reaction. The present experiments can detect fulvene with particular selectivity because it has the lowest photoionization energy of the C_6H_6 isomers and appears at photon energies where other reaction products are absent. It is not specified in the publication of Jones et al. whether inferior fits resulted from using isomers other than benzene and 1,3-hexadien-5-yne. As the reported maximum benzene yields are consistent with the benzene yields observed in the molecular beam experiments, the major discrepancy with the Jones et al. report is the fraction of fulvene. A composite photoionization spectrum has been simulated that is composed of 70% 1,3-hexadien-5-yne and 30% benzene (Fig. 11), the branching fractions reported by Jones et al. [23]. It is clear from the comparison of this simulated composite spectrum and the actual spectrum measured in this experiment, also shown in Fig. 11, that the product branching fractions resulting in the onset and shape of the measured spectrum are unequivocally different to the values observed by Jones et al.

Jones et al. also report a computational investigation into the C_2H + 1,3-butadiene reaction that corroborates their experimental components [23]. The computational branching fractions are reported from 0 to 45 kJ mol^{-1} collision energy. At lower collision energies, which would be more comparable to the current flow tube conditions, they predict that the benzene product increases in relative yield compared to the 1,3-hexadien-5-yne, (branching given in Table 2). Jones et al. outline two possible pathways to benzene formation, which are shown in Fig. 12, cyclization of the initial adduct followed by H-shift or H-shift followed by cyclization, both followed by H-loss to yield benzene; all values in Fig. 12 are reproduced from that paper. Jones et al. state that 99% of the benzene molecules are formed by the first pathway. 1,3-hexadien-5-yne can be formed *via* direct H-loss from the adduct formed by terminal addition of C_2H to 1,3-butadiene *via* a transition state that lies 13 kJ mol^{-1} higher in energy than the separated 1,3-hexadien-5-yne + H products. Jones et al. do not mention the possibility of any products other than benzene or 1,3-hexadien-5-yne and so it is difficult to know if formation of any other isomers was considered. From the computational studies carried out and presented here, the transition state with the highest energy in the proposed fulvene-formation pathway lies at −116 kJ mol^{-1} relative to the asymptote for the reactants, whereas the highest energy transition state on the 1,3-hexadien-5-yne -formation pathway of Jones et al.

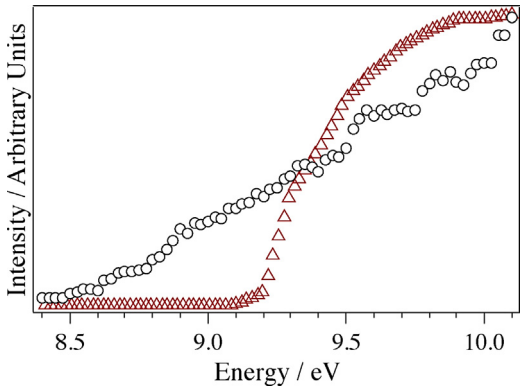

Fig. 11. Black circles show the measured photoionization spectrum for the products with $m/z = 78$ in the current experiment. Red triangles show a simulated spectrum with a composition of 70% 1,3-hexadien-5-yne and 30% benzene, the branching fractions reported by Jones et al. [23]. Both spectra are normalized to the same maximum value.

lies at -103 kJ mol^{-1}, a difference of 13 kJ mol^{-1}. It may be that this fulvene formation path may be able to effectively compete with the proposed 1,3-hexadien-5-yne formation path by Jones et al., and with the lower-energy benzene formation pathway shown in Fig. 12, depending on the entropy of each transition state and the effect of the collisional stabilization in our experiment.

All of the proposed 3,4-dimethylenecyclobut-1-ene pathways involve preliminary H-shifts, which, due to the lack of C_5H_4 products detected in the current experiment, have been postulated to be unfavorable, as discussed earlier. Furthermore, the assignment of 3,4-dimethylenecyclobutene is less definitive than the observation of fulvene formation (see above). Consequently, in the case of the 3,4-dimethylenecyclobut-1-ene product, further experimental or theoretical work would be particularly valuable to corroborate its formation. It is possible that lower energy pathways to both fulvene and 3,4-dimethylenecyclobut-1-ene exist that have not been found in the present calculations.

Although we observe no spectroscopic evidence for benzene, the signal-to-noise ratio in the photoionization spectrum indicates that benzene could account for a maximum of 45% of products of the C_2H + 1,3-butadiene reaction under the current conditions. The maximum branching fraction of 45% is in fair agreement with the

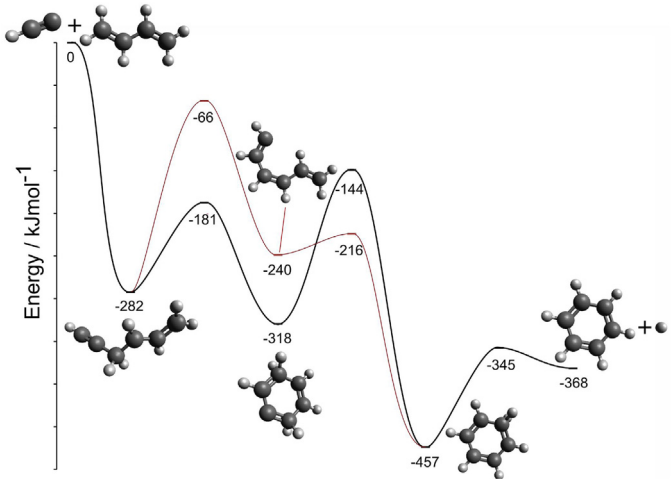

Fig. 12. Minima and first-order saddle points on two possible reaction pathways to benzene formation in the C_2H + 1,3-butadiene reaction. Values and structures are from the publication by Jones et al. [23].The thick black line shows the pathway that accounts for 99% of benzene products, according to Jones et al., and the thin red line shows the pathway that accounts for the remaining 1% of benzene products.

branching fractions measured (30% at 45 kJ mol^{-1} collision energy) and predicted (40% at 0 kJ mol^{-1} collision energy) by Jones et al. [23]. Given the significance of benzene in PAH chemistry in both astrochemical and combustion environments, it is important to identify reactions that are likely or unlikely to form benzene. Jones et al. propose that the C_2H + 1,3-butadiene reaction is a likely candidate for benzene production in the interstellar medium. However, the experimental evidence presented here suggests that the C_2H + 1,3-butadiene reaction may also contribute significantly to yields of the 5-membered ring species fulvene in such environments. It would be very interesting to search for the major product of the C_2H + 1,3-butadiene reaction, fulvene, in the interstellar medium as this molecule possesses a substantial dipole moment [66] and may be present as a result of the title reaction where C_2H radicals are abundant, for example in circumstellar shells.

One factor that would assist greatly in the interpretation of the photoionization spectrum would be accurate absolute photoionization spectra for 3,4-dimethylenecyclobut-1-ene, 3-methylene-1-penten-4-yne and 3-methyl-1,2-pentadien-4-yne. Alternatively, the system could be studied using different experimental methodologies, or current methodology could be augmented with a secondary component for identification. A full time-dependent, multi-well master equation investigation of this system, which includes the new pathways presented here, would be very valuable, particularly given the significance of the title reaction in formation of cyclic molecules in astrochemical and combustion environments.

5. Conclusion

The reaction of C_2H with 1,3-butadiene was investigated using a slow flow reactor at 4 Torr and 298 K coupled with synchrotron photoionization time-of-flight mass spectrometry. The primary channel in the reaction is H-loss from the adduct to yield C_6H_6. No signal is observed from the $C_5H_4 + CH_3$ channel, which is prominent when C_2H reacts with other C_4H_6 isomers, implying that the title reaction does not access the entrance channels involved in reaction with the other C_4H_6 isomers. The measured photoionization spectrum of this C_6H_6 product reveals that fulvene is formed with branching fraction of (57 ± 30)%. From the deviation of the measured spectrum from that of fulvene, it seems very likely that additional isomers of C_6H_6 are formed. Using the currently available calibration photoionization spectra for each isomer, maximum branching fractions for 3,4-dimethylenecyclobut-1-ene, 3-methylene-1-penten-4-yne and 3-methyl-1,2-pentadien-4-yne are calculated to be 74%, 24% and 31%, respectively. The upper limit of the branching fraction for the sum of benzene and 1,3-hexadien-5-yne under the current conditions is 45%. The observation of fulvene as the major product of the title reaction is not in good agreement with the interpretation of Jones et al. [23], suggesting that further investigation of the C_2H + 1,3-butadiene reaction would be valuable to better understand formation of cyclic species in combustion and astrochemical environments.

Several energetically feasible reaction pathways to fulvene and 3,4-dimethylenecyclobut-1-ene from the C_2H + 1,3-butadiene reactants have been determined using quantum chemical methods. For fulvene formation a route involving relatively low energy transition states has been calculated, which may be able to effectively compete with the benzene-formation pathway calculated by Jones et al. [23] under the current conditions. Given the potentially significant reaction channels and the disagreement encountered between studies thus far, a full time-dependent multi-well master equation calculation and further experimental investigation of the C_2H + 1,3-butadiene system would be extremely valuable.

Acknowledgements

S.R.L. and J.F.L. are supported by the Director, Office of Science, Office of Basic Energy Sciences of the U.S. Department of Energy under Contract DE-AC03-76SF0098 at Lawrence Berkeley National Laboratory. M.F. thanks the I.R.S. acknowledges the France Berkeley Fund and the Université de Rennes 1 and the France-Berkeley Fund for financial support to enable his stay at the Advanced Light Source. I.R.S. acknowledges the Université de Rennes 1. J.-C.G. thanks the Centre National d'Etudes Spatiales (CNES) for financial support. Sandia authors, and the development and maintenance of the multiplexed photoionization mass spectrometry kinetics experiment, were funded by the Division of Chemical Sciences, Geosciences, and Biosciences, the Office of Basic Energy Sciences (BES), United States Department of Energy (DOE). Sandia is a multiprogram laboratory operated by Sandia Corporation, a Lockheed Martin Company, for the National Nuclear Security Administration, under contract DE-AC04-94AL85000. The Advanced Light Source is supported by the Director, Office of Science, BES/DOE, under contract DE-AC02-05CH11231 between Lawrence Berkeley National Laboratory and the DOE.

Appendix A. Supplementary data

Supplementary data associated with this article can be found, in the online version, at http://dx.doi.org/10.1016/j.ijms.2014.08.025.

References

[1] L.M. Ziurys, The chemistry in circumstellar envelopes of evolved stars: following the origin of the elements to the origin of life, Proc. Natl. Acad. Sci. U. S. A. 103 (2006) 12274–12279.
[2] E.H. Wilson, S.K. Atreya, A. Coustenis, Mechanisms for the formation of benzene in the atmosphere of Titan, J. Geophys. Res. -Planets 108 (2003) .
[3] J.A. Cole, J.D. Bittner, J.P. Longwell, J.B. Howard, Formation mechanisms of aromatc-compounds in aliphatic flames, Combust. Flame 56 (1984) 51–70.
[4] J.A. Miller, C.F. Melius, Kinetic and thermodynamic issues in the formation of aromatic-compounds in flames of aliphatic fuels, Combust. Flame 91 (1992) 21–39.
[5] K.C. Smyth, J.H. Miller, Chemistry of molecular growth-processes in flames, Science 236 (1987) 1540–1546.
[6] J. Cernicharo, A.M. Heras, A. Tielens, J.R. Pardo, F. Herpin, M. Guelin, L. Waters, Infrared space observatory's discovery of C_4H_2, C_6H_2, and benzene in CRL 618, Astrophys. J. 546 (2001) L123–L126.
[7] S.E. Malek, J. Cami, J. Bernard-Salas, The rich circumstellar chemistry of SMP LMC 11, Astrophys. J. 744 (2012) .
[8] V. Vuitton, R.V. Yelle, J. Cui, Formation and distribution of benzene on Titan, J. Geophys. Res. -Planets 113 (2008) .
[9] P.R. Westmoreland, A.M. Dean, J.B. Howard, J.P. Longwell, Forming benzene in flames by chemically activated isomerization, J. Phys. Chem. 93 (1989) 8171–8180.
[10] N. Hansen, J.A. Miller, S.J. Klippenstein, P.R. Westmoreland, K. Kohse-Hoinghaus, Exploring formation pathways of aromatic compounds in laboratory-based model flames of aliphatic fuels, Combust. Explos. 48 (2012) 508–515.
[11] N.M. Marinov, W.J. Pitz, C.K. Westbrook, A.M. Vincitore, M.J. Castaldi, S.M. Senkan, C.F. Melius, Aromatic and polycyclic aromatic hydrocarbon formation in a laminar premixed *n*-butane flame, Combust. Flame 114 (1998) 192–213.
[12] W.Y. Tang, R.S. Tranter, K. Brezinsky, Isomeric product distributions from the self-reaction of propargyl radicals, J. Phys. Chem. A 109 (2005) 6056–6065.
[13] J.A. Miller, S.J. Klippenstein, The recombination of propargyl radicals and other reactions on a C_6H_6 potential, J. Phys. Chem. A 107 (2003) 7783–7799.
[14] J.J. Newby, J.A. Stearns, C.P. Liu, T.S. Zwier, Photochemical and discharge-driven pathways to aromatic products from 1,3-butadiene, J. Phys. Chem. A 111 (2007) 10914–10927.
[15] X. Lories, J. Vandooren, D. Peeters, Theoretical study of the C_6H_7 energy surface, Proc. Eur. Combust. Meeting (2009) .
[16] S.M. Sarathy, S. Vranckx, K. Yasunaga, M. Mehl, P. Osswald, W.K. Metcalfe, C.K. Westbrook, W.J. Pitz, K. Kohse-Hoinghaus, R.X. Fernandes, H.J. Curran, A comprehensive chemical kinetic combustion model for the four butanol isomers, Combust. Flame 159 (2012) 2028–2055.
[17] K.D. Tucker, M.L. Kutner, P. Thaddeus, The ethynyl radical C_2H – a new interstellar molecule, Astrophys. J. 193 (1974) L155–L199.
[18] H. Beuther, D. Semenov, T. Henning, H. Linz, Ethynyl (C_2H) in massive star formation: tracing the initial conditions? Astrophys. J. Lett. 675 (2008) L33–L36.
[19] E.H. Wilson, S.K. Atreya, Current state of modeling the photochemistry of Titan's mutually dependent atmosphere and ionosphere, J. Geophys. Res. -Planets 109 (2004) .
[20] A. Jamal, A.M. Mebel, An sb initio/RRKM study of the reaction mechanism and product branching ratios of the reactions of ethynyl radical with 1,2-butadiene, Chem. Phys. Lett. 518 (2011) 29–37.
[21] J.P. Fonfria, J. Cernicharo, M.J. Richter, J.H. Lacy, The abundances of polyacetylenes toward CRL618, Astrophys. J. 728 (2011) .
[22] P.M. Woods, T.J. Millar, E. Herbst, A.A. Zijlstra, The chemistry of protoplanetary nebulae, Astron. Astrophys. 402 (2003) 189–199.
[23] B.M. Jones, F.T. Zhang, R.I. Kaiser, A. Jamal, A.M. Mebel, M.A. Cordiner, S.B. Charnley, Formation of benzene in the interstellar medium, Proc. Natl. Acad. Sci. U. S. A. 108 (2011) 452–457.
[24] M. Mehl, W.J. Pitz, C.K. Westbrook, H.J. Curran, Kinetic modeling of gasoline surrogate components and mixtures under engine conditions, Proc. Combust. Inst. 33 (2011) 193–200.
[25] T. Tanzawa, W.C. Gardiner, Reaction-mechanism of the homogenous thermal-decomposition of acetylene, J. Phys. Chem. 84 (1980) 236–239.
[26] A. Jamal, A.M. Mebel, Reactions of C_2H with 1-and 2-Butynes: an ab initio/RRKM study of the reaction mechanism and product branching ratios, J. Phys. Chem. A 115 (2011) 2196–2207.
[27] S.B. Morales, C.J. Bennett, S.D. Le Picard, A. Canosa, I.R. Sims, B.J. Sun, P.H. Chen, A.H.H. Chang, V.V. Kislov, A.M. Mebel, X.B. Gu, F.T. Zhang, P. Maksyutenko, R.I. Kaiser, A crossed molecular beam low-temperature kinetics, and theoretical investigation of the reaction of the cyano radical (CN) with 1,3-butadiene (C_4H_6). A route to complex nitrogen-bearing molecules in low-temperature extraterrestrial environments, Astrophys. J. 742 (2011) .
[28] D. Chastaing, P.L. James, I.R. Sims, I.W.M. Smith, Neutral–neutral reactions at the temperatures of interstellar clouds – rate coefficients for reactions of C_2H radicals with O_2, $C_2H_2C_2H_4$ and C_3H_6 down to 15 K, Faraday Discuss. 109 (1998) 165–181.
[29] I.R. Sims, J.L. Queffelec, D. Travers, B.R. Rowe, L.B. Herbert, J. Karthauser, I.W.M. Smith, Rate constants for the reactions of CN with hydrocarbons at low and ultra-low temperatures, Chem. Phys. Lett. 211 (1993) 461–468.
[30] F. Stahl, P.V. Schleyer, H.F. Schaefer, R.I. Kaiser, Reactions of ethynyl radicals as a source of C-4 and C-5 hydrocarbons in Titan's atmosphere, Planet Space Sci. 50 (2002) 685–692.
[31] N. Balucani, O. Asvany, L.C.L. Huang, Y.T. Lee, R.I. Kaiser, Y. Osamura, H.F. Bettinger, Formation of nitriles in the interstellar medium via reactions of cyano radicals CN(X(2) Sigma(+)), with unsaturated hydrocarbons, Astrophys. J. 545 (2000) 892–906.
[32] S. Soorkia, C.L. Liu, J.D. Savee, S.J. Ferrell, S.R. Leone, K.R. Wilson, Airfoil sampling of a pulsed laval beam with tunable vacuum ultraviolet synchrotron ionization quadrupole mass spectrometry: application to low-temperature kinetics and product detection, Rev. Sci. Instrum. 82 (2011) .
[33] J. Bouwman, F. Goulay, S.R. Leone, K.R. Wilson, Bimolecular rate constant and product branching ratio measurements for the reaction of C_2H with ethene and propene at 79 K, J. Phys. Chem. A 116 (2012) 3907–3917.
[34] J. Bouwman, M. Fournier, I.R. Sims, S.R. Leone, K.R. Wilson, Reaction rate and isomer-specific product branching ratios of $C_2H + C_4H8$: 1-butene, cis-2-butene, trans-2-butene, and isobutene at 79 K, J. Phys. Chem. A 117 (2013) 5093–5105.
[35] F. Goulay, S. Soorkia, G. Meloni, D.L. Osborn, C.A. Taatjes, S.R. Leone, Detection of pentatetraene by reaction of the ethynyl radical (C_2H) with allene (CH_2CCH_2) at room temperature, Phys. Chem. Chem. Phys. 13 (2011) 20820–20827.
[36] S. Soorkia, A.J. Trevitt, T.M. Selby, D.L. Osborn, C.A. Taatjes, K.R. Wilson, S.R. Leone, Reaction of the C_2H radical with 1-butyne (C_4H_6): low-temperature kinetics and isomer-specific product detection, J. Phys. Chem. A 114 (2010) 3340–3354.
[37] C.F. Cullis, D.J. Hucknall, J.V. Shepherd, Studies of reactions of ethynyl radicals with hydrocarbons, Proc. R. Soc. London Ser. A-Math. Phys. Eng. Sci. 335 (1973) 525–545.
[38] S. Soorkia, C.A. Taatjes, D.L. Osborn, T.M. Selby, A.J. Trevitt, K.R. Wilson, S.R. Leone, Direct detection of pyridine formation by the reaction of CH (CD) with pyrrole: a ring expansion reaction, Phys. Chem. Chem. Phys. 12 (2010) 8750–8758.
[39] F. Goulay, D.L. Osborn, C.A. Taatjes, P. Zou, G. Meloni, S.R. Leone, Direct detection of polyynes formation from the reaction of ethynyl radical (C_2H) with Propyne (CH_3CCH) and Allene (CH_2CCH_2), Phys. Chem. Chem. Phys. 9 (2007) 4291–4300.
[40] D.L. Osborn, P. Zou, H. Johnsen, C.C. Hayden, C.A. Taatjes, V.D. Knyazev, S.W. North, D.S. Peterka, M. Ahmed, S.R. Leone, The multiplexed chemical kinetic photoionization mass spectrometer: a new approach to isomer-resolved chemical kinetics, Rev. Sci. Instrum. 79 (2008) 104103–104113.
[41] Z. Fangtong, K. Seol, R.I. Kaiser, a crossed molecular beams study of the reaction of the ethynyl radical (C_2H(X2Sigma+)) with allene (H_2CCCH_2(X1A1)), Phys. Chem. Chem. Phys. 11 (2009) 4707–4714.
[42] A.M. Tarr, O.P. Strausz, H.E. Gunning, Reactions of ethynyl radical 1. Hydrogen abstraction from alkanes, Trans. Faraday Soc. 61 (1965) 1946–1959.
[43] L.A. Bashford, H.J. Emeleus, H.V.A. Briscoe, The oxidation of chloroacetylene and bromoacetylene, J. Chem. Soc. (1938) 1358–1364.
[44] J. Berkowitz, Photoionization of CH_3OH, CD_3OH and CH_3OD – dissociative ionization mechanisms and ionic structures, J. Chem. Phys. 69 (1978) 3044–3054.

[45] M.J. Frisch, G.W., Trucks, H.B., Schlegel, G.E., Scuseria, M.A., Robb, J.R., Cheeseman, G., Scalmani, V., Barone, B., Mennucci, G.A., Petersson, H., Nakatsuji, M., Caricato, X., Li, H.P., Hratchian, A.F., Izmaylov, J., Bloino, G., Zheng, J.L., Sonnenberg, M., Hada, M., Ehara, K., Toyota, R., Fukuda, J., Hasegawa, M., Ishida, T., Nakajima, Y., Honda, O., Kitao, H., Nakai, T., Vreven, J., Montgomery, J. A., J.E. Peralta, F., Ogliaro, M., Bearpark, J.J., Heyd, E., Brothers, K.N., Kudin, V.N., Staroverov, R., Kobayashi, J., Normand, K., Raghavachari, A., Rendell, J.C., Burant, S.S., Iyengar, J., Tomasi, M., Cossi, N., Rega, J.M., Millam, M., Klene, J.E., Knox, J.B., Cross, V., Bakken, C., Adamo, J., Jaramillo, R., Gomperts, R.E., Stratmann, O., Yazyev, A.J., Austin, R., Cammi, C., Pomelli, J.W., Ochterski, R.L., Martin, K., Morokuma, V.G., Zakrzewski, G.A., Voth, P., Salvador, J.J., Dannenberg, S., Dapprich, A.D., Daniels, Ö., Farkas, J.B., Foresman, J.V., Ortiz, J., Cioslowski, D.J., Fox Gaussian 09, in: Gaussian Inc. , Wallingford CT, 2009.
[46] J.W. Ochterski, G.A. Petersson, J.A. Montgomery Jr., A complete basis set model chemistry. V. extensions to six or more heavy atoms, J. Chem. Phys. 104 (1996) 2598–2619.
[47] F. Santoro, R. Improta, A. Lami, J. Bloino, V. Barone, Effective method to compute Franck–Condon integrals for optical spectra of large molecules in solution, J. Chem. Phys. 126 (2007) 1–13.
[48] V. Barone, J. Bloino, M. Biczysko, F. Santoro, Fully integrated approach to compute vibrationally resolved optical spectra: from small molecules to macrosystems, J. Chem. Theory Comput. 5 (2009) 540–554.
[49] M. Bobeldijk, W.J. Vanderzande, P.G. Kistemaker, Simple models for the calculation of photoionization and electron-impact ionization cross-sections of polyatomic molecules, Chem. Phys. 179 (1994) 125–130.
[50] Y. Zhao, D.G. Truhlar, The M06 suite of density functionals for main group thermochemistry, thermochemical kinetics, noncovalent interactions, excited states, and transition elements: two new functionals and systematic testing of four M06-class functionals and 12 other functionals, Theor. Chem. Acc. 120 (2008) 215–241.
[51] J.A. Montgomery, M.J. Frisch, J.W. Ochterski, G.A. Petersson, A complete basis set model chemistry. VI. use of density functional geometries and frequencies, J. Chem. Phys. 110 (1999) 2822–2827.
[52] J.A. Montgomery, M.J. Frisch, J.W. Ochterski, G.A. Petersson, A complete basis set model chemistry. VII. Use of the minimum population localization method, J. Chem. Phys. 112 (2000) 6532–6542.
[53] P.T. Howe, A. Fahr, Pressure and temperature effects on product channels of the propargyl ($HCCCH_2$) combination reaction and the formation of the first ring, J. Phys. Chem. A 107 (2003) 9603–9610.
[54] T.A. Cool, J. Wang, K. Nakajima, C.A. Taatjes, A. McIlroy, Photoionization cross sections for reaction intermediates in hydrocarbon combustion, Int. J. Mass Spectrom. 247 (2005) 18–27.
[55] A.M. Tarr, O.P. Strausz, H.E. Gunning, Reactions of ethynyl radical 2. With alkenes, Trans. Faraday Soc. 62 (1966) 1221–1230.
[56] J.D. Savee, S. Soorkia, O. Welz, T.M. Selby, C.A. Taatjes, D.L. Osborn, Absolute photoionization cross-section of the propargyl radical, J. Chem. Phys. 136 (2012) 134307–134317.
[57] P. Hockett, E. Ripani, A. Rytwinski, A. Stolow, Probing ultrafast dynamics with time-resolved multi-dimensional coincidence imaging: butadiene, J. Mod. Opt. 60 (2013) 1409–1425.
[58] K. Bergmann, Demtrode.w mass-spectrometric investigation of primary processes in photodissociation of 1,3-butadiene, J. Chem. Phys. 48 (1968) 18–22.
[59] G.J. Collin, H. Deslauriers, G.R. Demare, R.A. Poirier, The 213.8 nm photochemistry of gaseous 1,3-Butadiene and the structure of some C_3H_3 radicals, J. Phys. Chem. 94 (1990) 134–141.
[60] J.C. Robinson, S.A. Harris, W.Z. Sun, N.E. Sveum, D.M. Neumark, Photofragment translational spectroscopy of 1,3-Butadiene and 1,3-Butadiene-1,1,4,4-d(4) at 193 nm, J. Am. Chem. Soc. 124 (2002) 10211–10224.
[61] R.D. Doepker, Vacuum-ultraviolet photolysis of C_4H_6 isomers. I. 1,3-Butadiene, J. Phys. Chem. 72 (1968) 4037–4042.
[62] D.L. Osborn, Personal Communication.
[63] P.J. Linstrom, W.G. Mallard, NIST Chemistry WebBook, in: Eds. (Ed.) NIST Standard Reference Database Number 69, National Institute of Standards and Technology, Gaithersburg MD.
[64] J.W. Ochterski, G.A. Petersson, J.A. Montgomery, A complete basis set model chemistry .V. Extensions to six or more heavy atoms, J. Chem. Phys. 104 (1996) 2598–2619.
[65] D. Mandal, B. Mondal, A.K. Das, The association reaction between C_2H and 1-butyne: a computational chemical kinetics study, Phys. Chem. Chem. Phys. 13 (2011) 4583–4595.
[66] G.W. Wheland, D.E. Mann, The dipole moments of fulvene and azulene, J. Chem. Phys. 17 (1949) 264–268.